ACS APPLIED MATERIALS & INTERFACES

Research Article

www.acsami.org

Highly Efficient Nanoarchitectured Ni_5TiO_7 Catalyst for Biomass Gasification

Xin Jiang,*[,†] Lei Zhang,[†] Swetlana Wybornov,[†] Thorsten Staedler,[†] Daniel Hein,[‡] Florian Wiedenmann,[‡] Wolfgang Krumm,[‡] Vladimir Rudnev,[§] and Irina Lukiyanchuk[§]

[†]Institute of Materials Engineering, University of Siegen, Paul-Bonatz-Str. 9-11, 57076 Siegen, Germany

[‡]Institute of Energy Technique, University of Siegen, Paul-Bonatz-Str. 9-11, 57076 Siegen, Germany

[§]Institute of Chemistry, Far East Division, Russian Academy of Sciences, Prosp. Stoletiya Vladivostoka 159, 690022 Vladivostok, Russia

Supporting Information

ABSTRACT: We report the synthesis of needle-shaped nanocrystals of Ni_5TiO_7 utilizing a solid-phase reaction of NiO with a porous and rough TiO_2 surface produced by plasma electrolytic oxidation. The single crystalline orthorhombic nanocrystals are grown along the [010] axis, featuring a length of ~10 μm and diameters varying from several tens of nanometers up to 200 nm. The resulted novel Ni_5TiO_7/TiO_2/Ti nanoarchitectured compound composite has been proven outstandingly active as a catalyst and appears most suitable for high-temperature operation in biomass gasification. The findings may pave the way to an improved and environmentally friendly technology of energy generation.

KEYWORDS: *nanostructured materials, Ni_5TiO_7/TiO_2/Ti compound composite, catalysis, biomass gasification, transmission electron microscopy*

1. INTRODUCTION

The climate debate in context of the expected shortage of fossil fuels has intensified the worldwide request for a more efficient use of existing fossil fuels, as well as the search for alternative energy sources. Biomass is one of those important alternative energy sources. By a forced gasification, biomass is transformed to syngas, which can be used as a gaseous fuel for electricity generation or as a feedstock for the synthesis of clean transportation fuels.[1] However, the most crucial problem in the biomass gasification process is the high tar content in the produced gas. Tar leads to the formation of aerosol as well as a potential deposition on surfaces of equipment inside the process such as gasifiers and engines or turbine systems that, in turn, will cause mechanical problems.[2] Tar contents in the produced gas could be significantly lowered by applying multistaged gasification concepts.[3] To obtain a gas quality suitable for a reliable operation of combustion engines, additional and costly gas cleaning is still necessary.

Over the past decades, catalytic steam reforming with minimal energy lost and without environmental contamination has attracted increasing interest as a promising technology for reducing tar. Several extensive investigations have been carried out utilizing either a model compound or real tar.[4−7] It was reported that catalysts, essentially nickel-based metallic and nonmetallic materials (mainly of mineral origin), showed significant drawbacks, in spite of their ability in reducing the amount of tar. One of the drawbacks is the coke deposition. Because of this, Ni-based catalysts only feature a high initial activity but become deactivated rapidly thereafter. Alkali metals can also be potentially used as catalysts. Unfortunately, these are deactivated easily by sintering. Rhodium (Rh)-supported catalysts have shown the best activity, stability, and selectivity for hydrogen production. However, Rh is too expensive to be economically applied in steam reformation of tar. Therefore, an inexpensive and efficient catalyst is still one of the limiting factors for the biomass gasification.[8]

Because of their high specific surface area, the use of nanomaterials is a popular path in order to achieve the highest functional efficiency as catalytic material. Even though the syntheses and subsequent investigations of properties of novel nanotubes and nanowires have vigorously been pursued in the past decade, because of their great application potential in various technological branches,[9] no investigations of in situ synthesis of novel nanowires in the field of catalyzing gas products with biomass gasification have been performed. The reason for this most likely lies in the complex materials preparation in combination with associated high costs. A few attempts with catalysts in the form of nanoparticles have been

Received: May 14, 2012
Accepted: July 10, 2012
Published: July 10, 2012

carried out. Typically, the particles were simply impregnated, but not chemically bonded, on a supporting material.[10] The spherical geometry of the catalysts allows for an increase of the specific surface area, but only with a limited amount of mass.

In this paper, we report the synthesis of the novel nanoarchitectured $Ni_5TiO_7/TiO_2/Ti$ compound composite and its performance as a catalyst in a biomass gasification process. The in situ grown, thin Ni_5TiO_7 needles have proven outstandingly active as catalysts and appear most suitable for high-temperature operation in biomass gasification featuring high efficiency and long-term stability. This finding is of great interest for gasification of biomass in the context of energy generation and may pave the way to an improved and environmentally friendly technology.

2. EXPERIMENTAL SECTION

A new but simple two-step process was developed to prepare the $Ni_5TiO_7/TiO_2/Ti$ compound composite. In contrast to already reported procedures, which used either template-based or cost-intensive micro- and photolithography techniques, the compound nanocrystals presented here were grown by annealing of pre-prepared compound materials in an air atmosphere. The starting material was a (NiO + CuO)/TiO_2/Ti composite. Cylindrical titanium supporting material (diameter ⌀ = 2 mm; length L = 330 mm) was first plasma-electrolytically oxidized (PEO), which resulted in the formation of a porous TiO_2 surface layer with electrolyte element incorporation. This procedure was followed by an impregnation in a solution of nickel and copper salts and a final heating step in air at 500 °C to form a NiO and CuO_x crystallite mixture attached to the TiO_2 surfaces (Figure 1). It is speculated that

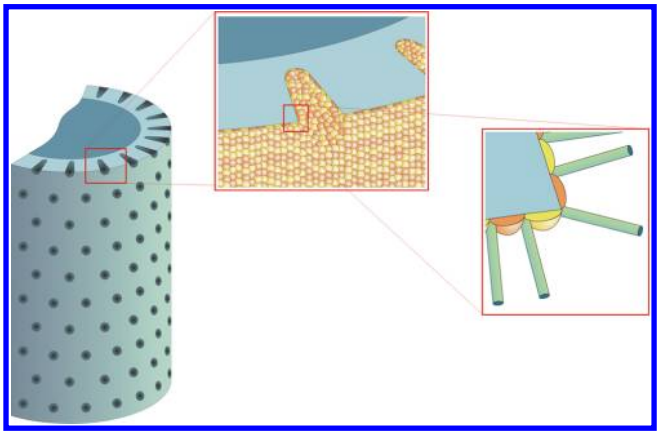

Figure 1. Manufacture procedure of (NiO + CuO)/TiO_2/Ti composites. In a first step, plasma-electrolytically oxidized (PEO) porous TiO_2 surface layer is formed on a Ti support. Then, NiO + CuO crystals are formed via the impregnation of nickel and copper salts, followed by heating in air. Finally, needle crystals of Ni_5TiO_7 are grown. The strongly reduced portion of CuO on the TiO_2 surface is attributed to a thermal diffusion.

the CuO_x crystallites act as spacers limiting the connection area between NiO and TiO_2 and further controlling the diameter of later-formed nanocrystals. After cutting the final rods into pieces featuring a length of L = 10 mm, which makes them most suitable for biocatalyzing applications, the growth of novel Ni_5TiO_7 nanoneedles was realized by in situ annealing of the oxide composites in an air atmosphere at temperatures between 650 °C and 950 °C. The duration of the annealing process lasted a couple of hours, depending on the actual growth temperature.

3. RESULTS AND DISCUSSION

The developed process, shown in Figure 1 and discussed in detail in the Supporting Information, results in low-cost, production-friendly nanoarchitectured catalysts that feature high efficiency and long-term stability. Catalysts on metal supports generally offer many advantages in a catalyzing process. They typically show good heat conduction; thereby, it is possible to dissipate local excess heat. Furthermore, they are mechanically stable and can easily be processed with different shapes of the catalyst block.[11]

The needle-shaped nanocrystals of Ni_5TiO_7 that were grown on the porous TiO_2 surface within 1 h at 900 °C featured a length of ∼10 μm and diameters varying from several tens of nanometers up to 200 nm, as presented in the SEM images of Figures 2 and 3a. The high-density nanowires were grown from

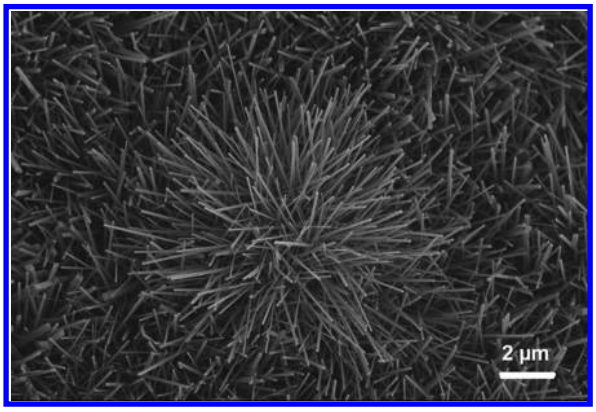

Figure 2. SEM image of the as-prepared needle crystals of Ni_5TiO_7.

the substrate surface with variable angles (Figure 2) and have a prism-like morphology. It was found that the growth of the title nanocrystals starts at a temperature of ∼650 °C, reaching its highest growth rate at 750−800 °C.

A bright-field TEM image of a part of an as-grown single nanocrystal, showing a wire width of 50 nm, and its corresponding selected area diffraction pattern, are shown in Figures 3b and 3c, respectively. The longitudinal direction of the nanocrystal indicated by "u" is parallel to the v-direction of the diffraction pattern. After careful analysis, those nanocrystals are verified to be single crystalline orthorhombic Ni_5TiO_7 with lattice constants of $a \approx 0.920$ nm, $b \approx 0.299$ nm, and $c \approx 1.217$ nm, respectively. By tilting the crystal around its axis (i.e., along the u-direction), other diffraction patterns could be obtained. The diffraction patterns in Figure 3c−e were recorded along the $[10\bar{1}]$, $[20\bar{1}]$, and $[30\bar{1}]$ zone axes realized by turning the crystal around "u". It is demonstrated that the [010] direction (v) of the crystal remains unchanged. Consequently, it can be concluded that the axial growth direction of these nanocrystals is along the short axis of [010], $b \approx 0.299$ nm.

To explore the atomic structure, we performed a detailed high-resolution TEM (HRTEM) study of the nanocrystals. Figure 3f shows a typical image at an edge area recorded along the [100] zone axis. The two sets of intersecting lattice fringes, (002) and (010), are 0.608 and 0.299 nm distances apart, respectively. The [010] crystal growth direction is also indicated, parallel to the side face. It is apparent from that

dx.doi.org/10.1021/am3008449 | ACS Appl. Mater. Interfaces 2012, 4, 4062−4066

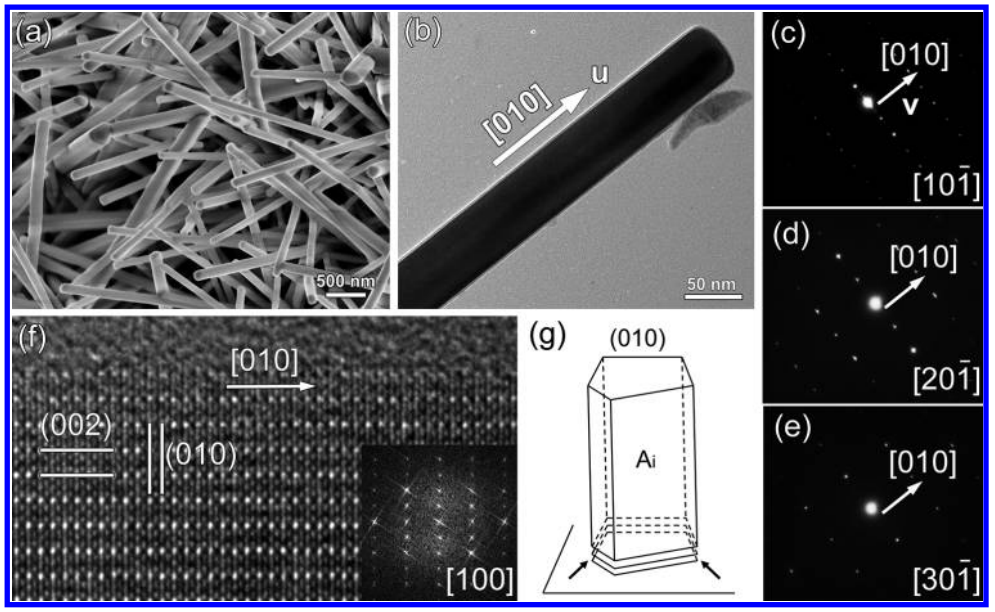

Figure 3. (a) SEM and (b) [10$\bar{1}$] zone-axis bright-field TEM images of the as-prepared needle crystals of Ni_5TiO_7. (c–e) Selected-area electron diffraction patterns recorded by tilting around the [010] axis from the specimen as shown in panel b. (f) High-resolution TEM image taken from the [100] zone axis of Ni_5TiO_7, and (g) schematic of the proposed growth model.

image that we are looking at a perfect crystal lattice without any defects such as dislocations or stacking faults. The Fourier transform diffraction pattern was easily obtained from the lattice image and is shown in the inset of Figure 3f.

In addition to the characterization by electron microscopy, quantitative evidence of the presence of Ni, Ti, and O in the nanowires was determined by energy-dispersive X-ray (EDX) analysis using both SEM and TEM systems focusing on the individual nanocrystals (see Figure 4). A small spot size (<3 nm

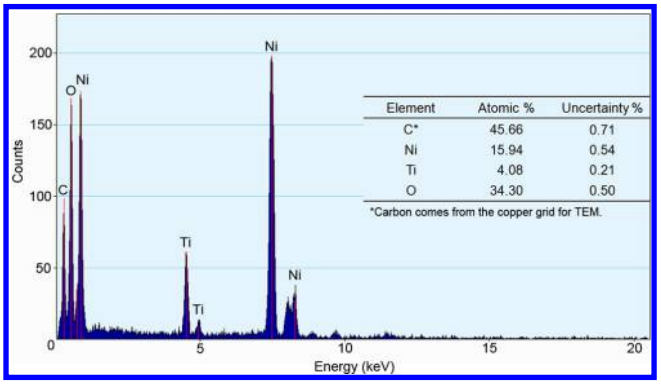

Figure 4. TEM-EDX spectrum of the Ni_5TiO_7 nanowire.

in TEM) was used to ensure that solely one nanocrystal contributes to the resulting information. The chemical composition obtained from the nanocrystals confirmed that only Ni, Ti, and O exist inside the crystal with an atomic ratio corresponding approximately to that of Ni_5TiO_7. Significant amounts of copper or other impurities were not detected by the analysis within the sensitivity limits. In addition, it was observed by EDX that the portion of CuO on the TiO_2 surface, due to thermal diffusion, was strongly reduced.

It can clearly be seen in the SEM image of Figure 3a that all nanocrystals are straight, individually featuring constant diameters. They show a faceted appearance of their sidewall surfaces. The shapes of wire cross-sections are not uniform. From the shapes of the crystallite ends/heads (equal to their cross sections) of the wires, one can estimate that the sidewall faces, A_i (i = 1, 2, 3, ...) in Figure 3g, of the nanocrystals parallel to the [010] crystal growth direction are the ($h0l$) planes, most likely the low-index (100), (001), (101), (102), (201), (103), and (203) planes.

According to the characterization presented above, a preferential growth of Ni_5TiO_7 nanocrystals along the [010] axis is proposed as the result of a strong growth competition of the (010) surface against other low-indexed planes of the sidewall faces. The crystal nucleation and growth, following the reaction

$$5NiO + TiO_2 = Ni_5TiO_7 \quad (1)$$

occur at the triple points on the interface between NiO and TiO_2 crystals. Because of its crystal lattice planes of particularly small d-values, the (010) plane exhibits less atomic packing density, possessing high surface energies so that the Ni_5TiO_7 nanocrystals are inclined to start growing in the [010] crystal direction, as shown in Figure 3g. Consequently, the high-energy (010) face will act as a growth face and the nanocrystals grow by being stacked up with plane-by-plane incorporation on the growth interface at the bottom of the wires on porous TiO_2 of the substrate (Figure 3g). The straight needlelike crystals are a result of local nucleation due to the CuO area separation and the molecular transport of the reaction pairs along the surfaces of the TiO_2 and NiO crystals (see Figure 3g).

The important role of CuO_x particles in the catalyst growth process has always been observed for the formation of Ni_5TiO_7 nanocrystals. We believe that the CuO_x crystallites act as spacers to organize the contact between NiO and TiO_2, to support local nucleation and, furthermore, to control the shape of the emerging nanocrystals. Once the nuclei of nanocrystals are formed they grow through the molecular transport of the reaction pairs along the surfaces of the TiO_2 and NiO crystals (Figure 3g) while CuO_x leaves the surface by thermal diffusion into the interior of the porous layer. Further analysis shows that the content of copper in the surface decreases while the total

concentration of copper in the whole layers remains constant, confirming this process.

Until now, no report about the synthesis of Ni_5TiO_7 nanowires exists. The successful synthesis of Ni_5TiO_7 macrocrystals with approximately submillimeter dimensions was first reported in 1976,[12] while $NiTiO_3$ had been recognized as the only stable compound in the $NiO-TiO_2$ system. After Shimura's report, only a few further investigations on related systems like $Ni_5TiB_2O_{10}$[13] have been reported. A possible reason for this might lie in the high formation temperature (over 1200 °C) of pure Ni_5TiO_7 crystals. It is nowadays widely accepted that nanosized crystals likely require lower activation energy of phase transformation, because of their large specific surface and the total system energy. In this context, the surface topography of the system discussed here featuring roughness and voids on the nanometer scale can lead to a reduction of the temperature for a reaction between NiO and TiO_2. The Ni_5TiO_7 crystal has the space group of C_{2v}^8-Pc2a, a density of 5.14 g/cm^3, and a melting point of ~1565 °C.[12]

Finally, the catalytic properties as well as the regeneration behavior of the self-supported $Ni_5TiO_7/TiO_2/Ti$ nanoarchitectured compound composites were tested. A laboratory-scale experimental plant was used, utilizing naphthalene as model tar. Nitrogen was used as a carrier gas and for inertization, while catalyst regeneration was realized using a mixture of nitrogen and oxygen. For the experimental arrangement, please see the Supporting Information.

The conversion–temperature ($C-T$) characteristics of the Ni_5TiO_7 nanowires confirmed the expected high efficiencies at high temperatures. Conversion as plotted in Figure 5 was determined according to

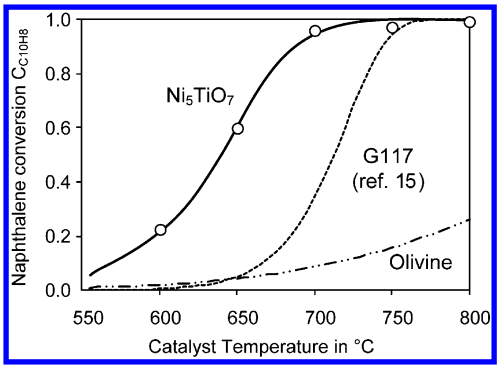

Figure 5. $C_{10}H_8$ conversion on G117 commercial Ni-catalyst (dotted line), on olivine (dash-dotted line), and on $Ni_5TiO_7/TiO_2/Ti$ compound system (empty circles are data points; trend is represented by the solid line). Residence time with respect to the empty reactor: 1.0 s (20 °C); atmospheric pressure; gas composition at reactor inlet: 1.7 vol % $C_{10}H_8$, 30 vol % H_2O, balance N_2.

$$C_{\text{gravimetric}} = \frac{m_{\text{tar,in}} - m_{\text{tar,out}}}{m_{\text{tar,in}}} \quad (2)$$

where $m_{\text{tar,in}}$ is the mass of tar evaporated and fed into the catalyst reactor and $m_{\text{tar,out}}$ is the mass of the solid residues determined by gravimetric analysis of the gas scrubbing solvent in the tar sampling impinge train.

Furthermore, a comparison to state-of-art materials like the Ni-based catalyst G117 (Südchemie AG, Munich, Germany) shows the good tar conversion activity of the title material. The catalyst G117 was originally developed for petrochemical processes. But since the steam reforming of naphthalene covers somewhat similar reaction networks, heavy hydrocarbon reforming catalysts are suitable for research in this field.

At 650 °C, the title material features a $C_{10}H_8$ conversion of ~60%. Under comparable experimental conditions and at a reactor temperature of 700 °C, gravimetric $C_{10}H_8$ conversion of ~30% for G117 and ~90% for the title compound system was determined; that is approximately three times the effectiveness of G117, which is a well-examined catalyst for biomass tar destruction,[14,15] and nine times the conversion efficiency of olivine, which is a well-investigated catalytically active bed material for biomass gasification reactors[16−18] (Figure 5). At 750 °C, almost-complete conversion has been achieved with our title compound. The dotted line in Figure 5 has been calculated from data given in ref 15. It should be mentioned that the experiments presented there were performed at a higher pressure of 160 kPa, lower naphthalene concentrations (0.4 vol %), and in the presence of H_2 (25 vol %). In addition, it is necessary to mention that a standard for tar sampling from producer gas was established first in 2006[19] and results obtained before that date may vary to a certain extent.

It is assumed that the increased specific surface of the architectured nanowires, compared to common coated spherical geometries, enhances naphthalene conversion. For the application as a downstream catalyst, the examined material appears very suitable, in terms of conversion efficiency and durability.

One remarkable point is the fact that tar conversion rates are rising during the first hours of operation until the full activity of the title catalyst system is established. Beginning with relatively poor tar conversion at the beginning, phenomena that are still to be investigated then lead to a rise in activity allowing for tar reforming activities up to an extent that basically no more gravimetric tar is detectable when applying a widely used and agreed upon tar sampling protocol.[19] Assuming a first-order kinetic approach with an effective conversion rate constant $k_{\text{m,tar}}$, according to eq 3, different catalysts can be compared concerning the temperature dependency of naphthalene conversion in an Arrhenius' plot (see Figure 6).

$$k_{\text{m,tar}} = -\left[\frac{\ln(1 - C_{\text{gravimetric}})}{\tau}\right] = k_{\text{m,tar,0}} \exp\left(-\frac{E_{\text{A,tar}}}{RT_{\text{cat}}}\right) \quad (3)$$

where

$\tau = m_{\text{cat}}/V_{\text{eff}}(T_{\text{cat}})$
$k_{\text{m,tar}}$ = conversion rate constant (in m^3/(kg$_{\text{cat}}$ h))
$k_{\text{m,tar,0}}$ = frequency factor (in m^3/(kg$_{\text{cat}}$ h))
τ = residence time (in (kg$_{\text{cat}}$ h)/m^3)
m_{cat} = mass of catalyst (in kg)
$V_{\text{eff}}(T_{\text{cat}})$ = volumetric gas flow in m^3/s

It becomes obvious that the advantage of the title system over reference catalysts increases with lower temperatures. Because of somewhat different experimental conditions, the plotted data for G117 should be read as a rough trend. Nevertheless, our results strengthen the conclusion that the naphthalene reforming performance of our Ni_5TiO_7 system is remarkably higher than that of other already investigated catalysts.

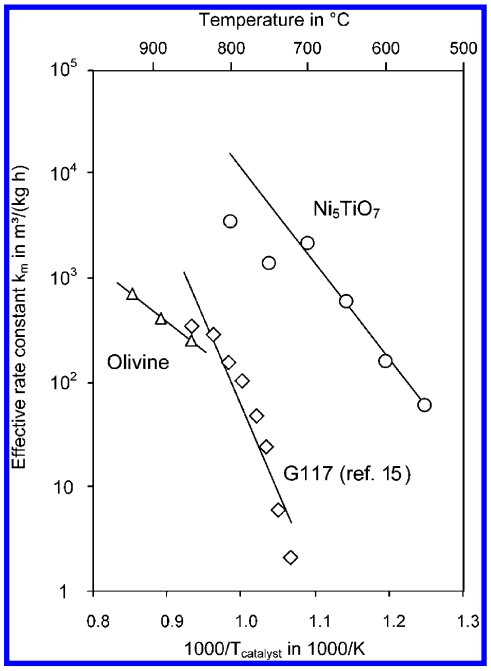

Figure 6. $C_{10}H_8$ conversion on (◇) G117 commercial Ni Catalyst, (△) olivine, and (○) Ni_5TiO_7/TiO_2/Ti compound system. Residence time with respect to the empty reactor: 1.0 s (20 °C); atmospheric pressure; gas composition at reactor inlet: 1.7 vol % $C_{10}H_8$, 30 vol % H_2O, balance N_2.

4. CONCLUSIONS

In this work, we succeeded in the synthesis of a further member of the compound nanowire family utilizing a solid reaction of NiO with a porous and atomically rough TiO_2 surface that has been produced by plasma oxidation. Outstanding catalytic properties for the steam reforming of naphthalene could be shown with a high stability even after 100 cycles of loading for 1 h with subsequent combustion of the coke residues arising from the reform. The gas yields of H_2, CO, and CH_4 in the reforming of naphthalene in the temperature range of 700−900 °C have been increased significantly by more than a factor of 2, compared to a commercial catalyst (G117).

These findings are supposed to be particularly important for future applications in the areas of gas cleaning and appropriate upgrading in the context of gasification of biogeneous and refuse-derived fuels.

■ ASSOCIATED CONTENT

Ⓢ Supporting Information

Details of the experimental methods. This material is available free of charge via the Internet at http://pubs.acs.org.

■ AUTHOR INFORMATION

Corresponding Author

*E-mail: xin.jiang@uni-siegen.de.

Notes

The authors declare no competing financial interest.

■ REFERENCES

(1) Han, J.; Kim, H. *Renew. Sust. Energy Rev.* **2008**, *12*, 397−416.
(2) Asadullah, M.; Miyazawa, T.; Ito, S.-i.; Kunimori, K.; Tomishige, K. *Appl. Catal., A* **2003**, *246*, 103−116.
(3) Hamel, S.; Hasselbach, H.; Weil, S.; Krumm, W. *Energy* **2007**, *32*, 95−107.
(4) Takanabe, K.; Aika, K.-i.; Inazu, K.; Baba, T.; Seshan, K.; Lefferts, L. *J. Catal.* **2006**, *243*, 263−269.
(5) Iojoiu, E. E.; Domine, M. E.; Davidian, T.; Guilhaume, N.; Mirodatos, C. *Appl. Catal., A* **2007**, *323*, 147−161.
(6) Tomishige, K.; Kimura, T.; Nishikawa, J.; Miyazawa, T.; Kunimori, K. *Catal. Commun.* **2007**, *8*, 1074−1079.
(7) Swierczynski, D.; Courson, C.; Kiennemann, A. *Chem. Eng. Process.* **2008**, *47*, 508−513.
(8) Park, H. J.; Park, S. H.; Sohn, J. M.; Park, J.; Jeon, J.-K.; Kim, S.-S.; Park, Y.-K. *Bioresour. Technol.* **2010**, *101*, S101−S103.
(9) Wang, Z. L. *Nanowires and Nanobelts—Materials, Properties and Devices; Vol. II: Nanowires and Nanobelts of Functional Materials*; Kluwer Academic Publishers: Boston, MA, 2003.
(10) Kim, J.-R.; Myeong, W.-J.; Ihm, S.-K. *Appl. Catal., B* **2007**, *71*, 57−63.
(11) Ganley, J. C.; Riechmann, K. L.; Seebauer, E. G.; Masel, R. I. *J. Catal.* **2004**, *227*, 26−32.
(12) Shimura, F.; Kawamura, T. *Jpn. J. Appl. Phys.* **1976**, *15*, 1403−1404.
(13) Armbruster, T.; Lager, G. A. *Acta Crystallogr., Sect. C: Cryst. Struct. Commun.* **1985**, *41*, 1400−1402.
(14) Jess, A. *Chem. Eng. Process.* **1996**, *35*, 487−494.
(15) Depner, H.; Jess, A. *Fuel* **1999**, *78*, 1369−1377.
(16) Świerczyński, D.; Courson, C.; Bedel, L.; Kiennemann, A.; Vilminot, S. *Chem. Mater.* **2006**, *18*, 897−905.
(17) Devi, L.; Ptasinski, K. J.; Janssen, F. J. J. G.; van Paasen, S. V. B.; Bergman, P. C. A.; Kiel, J. H. A. *Renew. Energy* **2005**, *30*, 565−587.
(18) Kuhn, J. N.; Zhao, Z.; Felix, L. G.; Slimane, R. B.; Choi, C. W.; Ozkan, U. S. *Appl. Catal., B* **2008**, *81*, 14−26.
(19) *Biomass gasification—Tar and particles in product gases—Sampling and analysis*; Standard DIN CEN/TS 15439, 2006.